Novel Lumped-Element Uniplanar Transitions

Yo-Shen Lin and Chun Hsiung Chen, *Fellow, IEEE*

***Abstract*—Novel reduced-size lumped-element uniplanar transitions are proposed, using the planar parallel and series inductor–capacitor (*LC*) circuits to realize the effective open and short circuits, respectively. In this study, various compact lumped-element coplanar waveguide-to-slotline and finite-ground coplanar waveguide-to-coplanar stripline transition structures are developed and carefully examined. Specifically, the performance of proposed basic lumped-element transitions can easily be adjusted through the control of L and C values, while the design of lumped-element Marchand-balun-type transitions may be accomplished by the use of conventional filter synthesis techniques. Simple equivalent-circuit models are also established, from which the passband behavior of the lumped-element transition structures may be characterized.**

***Index Terms*—Coplanar stripline, coplanar waveguide, Marchand balun, slotline, transition.**

I. Introduction

UNIPLANAR lines such as coplanar waveguides (CPWs), slotlines, and coplanar striplines (CPSs) have received increased attention due to their exclusive features over the conventional microstrip lines [1]. Modified uniplanar line structures, whether asymmetrical, finite-ground-plane, or conductor-backed, are also proposed and widely discussed in literature [2], [3]. These modifications introduce more control over the line characteristics as well as more design flexibility for uniplanar monolithic microwave integrated circuits (MMICs).

Among the uniplanar lines, the CPW has the advantage of easy integration with solid-state devices; however, it suffers a disadavantage due to the excitation of the parasitic odd CPW (or coupled slotline) mode at the discontinuities such as CPW bending, thus additional air-bridges/bondwires are needed that complicate the fabrication process. The slotline has the disadvantages of low Q and high radiation loss, and it is difficult to mount devices in series configuration; however, it is a good candidate for broad-band antenna applications. The CPS line with a balanced configuration may feature better immunity to power supply noise and ground noise than the unbalanced CPW and has the advantages of low discontinuity parasitics, less influence of spurious modes, and smaller area.

By taking the advantages of uniplanar structures, many microwave circuit components such as filters, couplers, balanced mixers, and antenna feeding structures have been developed [4]–[7]. These studies provide a variety of choices for the uniplanar MMIC designer such that maximum circuit integration and optimal system performance may be expected. To fully utilize the advantages of uniplanar lines and circuit components in a uniplanar MMIC system, implementation of broad-band, low loss, and compact interconnections between these uniplanar lines is of practical significance.

Various uniplanar transitions have been proposed and investigated, and the transition between the CPW and slotline has been studied most comprehensively. Most of the previous work on CPW-to-slotline transition design focused on the bandwidth improvement. In [8], the authors experimentally compared various transition structures and found that the transition that made use of a slotline-radial-open with radius of a quarter-wavelength ($\lambda/4$) had a wider bandwidth of 5.5 : 1. The transition utilized a complex combination of multiple $\lambda/4$-stub structures [9] which is attractive in improving the transition bandwidth even up to 160% (corresponding to the 10-dB return loss). The ideally all-pass double-Y junction transition [10] used a slotline-circular-open which not only occupies a large area but also limits its bandwidth. The transition employing the CPW-slotline mode-conversion phenomenon [11] was achieved by adding a 180° electrical delay to one slot of the CPW. All the transitions described above occupy large circuit area and lead to the inefficient use of high-cost substrate and active layers. Furthermore, the broad-band slotline-radial-open transition in [8] also suffers from the disadvantage of high radiation loss, which means that the spacing between the transition and other components in a circuit must be large enough to avoid crosstalk problems.

Only a few studies were reported with the goal of implementing compact CPW-to-slotline transitions. The Marchand-balun-type transition [9] realized with a $\lambda/4$ CPW series open stub printed on the CPW center conductor may save one air bridge and one-half of the circuit space; however, the transition size is still quite large due to the presence of another $\lambda/4$ shorted stub structure. The twin-spiral CPW-to-slotline transition [12] utilizes the spiral line structures such that 1/3∼1/4 the size of conventional transitions can be achieved, but a full-wave simulation is needed in part to characterize the transition performance.

Previous work on CPW-to-CPS transitions is relatively limited. The ideally all-pass double-Y junction balun [10] suffers from the junction parasitic effects, which lead to a limited operation bandwidth. The transition based on a $\lambda/4$ transformer structure [13] occupies large circuit area and is not suitable for use in the design of a MMIC, especially in the low-frequency range. The transition utilizing a slotline-open structure [14] has a very broad bandwidth, but no explicit design formulas are available to predict its upper passband frequency. Also, it has the drawback of higher power losses because the slotline-open structure would act as a radiated element.

Manuscript received March 28, 2001; revised August 11, 2001. This work was supported by the Ministry of Education and National Science Council of Taiwan under Grant 89-E-FA06-2-4 and under Grant NSC 89-2219-E-002-045.

The authors are with the Department of Electrical Engineering and Graduate Institute of Communication Engineering, National Taiwan University, Taipei 106, Taiwan, R.O.C. (e-mail: chchen@ew.ee.ntu.edu.tw).

Publisher Item Identifier S 0018-9480(01)10462-X.

In this study, a novel class of reduced-size lumped-element uniplanar transitions is proposed and investigated, which provides an easy and effective way of interconnection between unbalanced and balanced uniplanar lines. Specifically, planar lumped-element LC circuits are employed to replace the conventional $\lambda/4$ transformer structures. Therefore, the transition size may largely be reduced, and the transition passband frequency and bandwidth can be predicted and adjusted. Based on this concept, several lumped-element CPW-to-slotline and finite-ground coplanar waveguide (FGCPW)-to-CPS transitions are implemented and investigated. These transitions have the merits of compact size, low loss, and moderate bandwidth and thus may easily be incorporated into a uniplanar MMIC. The performance of these lumped-element transitions is easily adjusted by a selection of the L and C values and through the use of conventional filter synthesis techniques. To provide effective design tools, simple equivalent-circuit models are also established.

II. Basic Lumped-Element CPW-to-Slotline Transition Structures

Consider the basic lumped-element CPW-to-slotline transition structure [see Fig. 1(a)] proposed in [15]. To reduce the transition size, a planar parallel LC circuit composed of an interdigital structure and a shorted slotline stub is utilized to replace the conventional $\lambda/4$ transformer structure. The interdigital structure can be viewed as a capacitor as long as its size is much smaller than the wavelength. The capacitance is formed between each interdigital gap and is proportional to the length of finger and the ratio between finger width and gapwidth. The shorted slotline stub is equivalent to an inductor when its length is much smaller than the wavelength. This planar parallel LC circuit is connected to one slot of the CPW line in a shunt configuration and gives an effective open circuit at $f_0 = 1/(2\pi\sqrt{LC})$, which determines the center frequency of the transition passband. For suppressing the odd CPW (or coupled slotline) mode excited at the CPW–slotline junction, bondwires are included in the transition structure. One of the bondwires should be placed as close to the CPW–slotline junction as possible, with the others along the CPW line with a separation of about $\lambda/8$.

The capacitance of an interdigital capacitor is computed by the closed-form expressions under quasi-static approximation [16]. The capacitance per-unit length between each gap is first calculated using the conformal mapping technique. These per-unit length capacitances are multiplied by the finger length and are then added together to give the total capacitance. The available closed-form expressions enable a fast and simple characterization of the interdigital capacitor and are feasible for design purpose.

For the shorted slotline stub section, the detailed effect of the shorted end must be taken into account to accurately model the effective inductance value. Several full-wave analyses discovered that the end reactance is inductive and increases with the increase of slot width and the substrate-thickness-to-wavelength ratio [1]. In addition, the surface-wave and space-wave losses associated with the shorted end can be significant at high frequencies. These loss effects may be represented by an equivalent resistance. Since no closed-form formulas are available for these elements, here we use the full-wave mixed-potential integral-equation analysis [4] to simulate the input impedance Z_L of the shorted slotline end. In this full-wave simulation, the conductor is assumed to be perfectly conducting and of zero thickness, and the dielectric loss is not included in the calculations. The shorted slotline section may then be modeled by a transmission line terminated by an impedance Z_L, which would supply the desired effective inductance value.

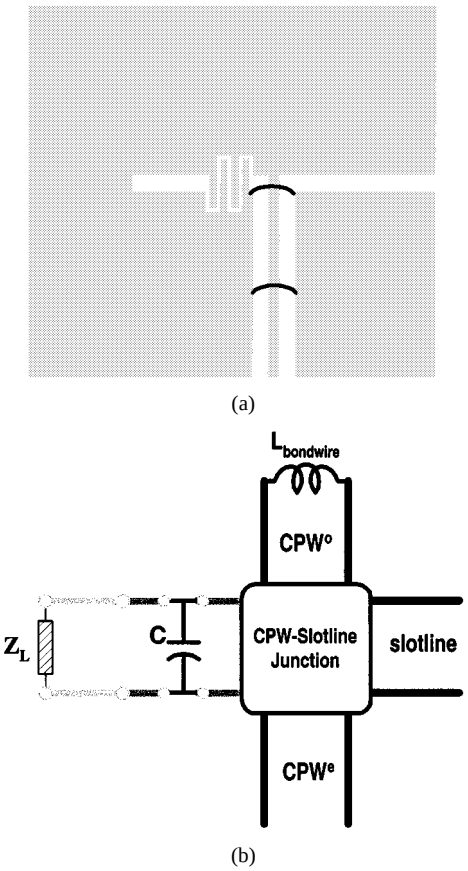

Fig. 1. Basic lumped-element CPW-to-slotline transition: (a) layout and (b) equivalent-circuit model.

Regarding the CPW-slotline T-junction, the three-port equivalent-circuit model [17] is adopted. In this model, the CPW line is represented by two transmission lines that separately support the even CPW mode and the odd CPW mode so as to describe the mode conversion effect at the junction. Specifically, bondwires are modeled as inductors and are connected to the odd CPW mode transmission line at their corresponding positions. The effect of imperfect suppression of the odd CPW mode can then be suitably modeled.

By combining the above-mentioned models, one may obtain the transmission-line equivalent-circuit model for the basic lumped-element CPW-to-slotline transition [see Fig. 1(a)] as in Fig. 1(b). This model is based on three assumptions. First, the CPW and slotline sections are modeled as transmission lines despite the non-TEM nature of slotline. Second, the detailed discontinuity effect of the CPW–slotline T-junction is neglected. Third, the interactions between the lumped-element LC circuit and the transmission lines are not taken into account.

A back-to-back lumped-element CPW-to-slotline transition for Fig. 1(a) is fabricated on the FR4 substrate (dielectric con-

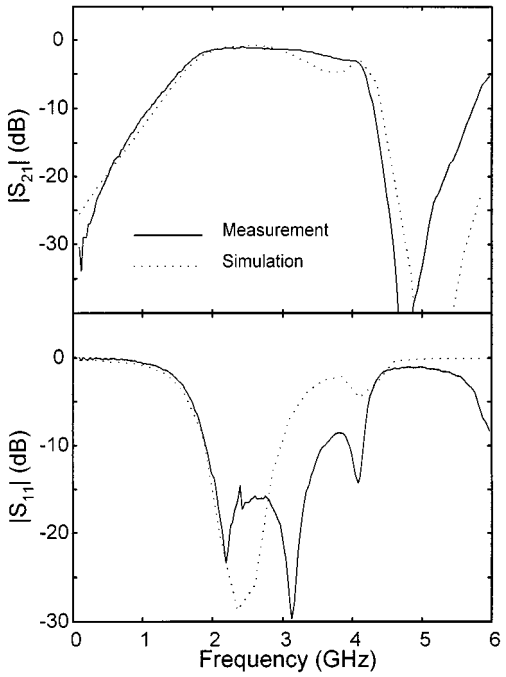

Fig. 2. Measured and simulated results for the back-to-back lumped-element CPW-to-slotline transition shown in Fig. 1(a).

stant $\varepsilon_r = 4.3$, loss tangent $\tan\delta = 0.022$, and thickness $h = 1.6$ mm). The CPW line has a strip width of 0.75 mm and a slot width of 1 mm. The slotline line has a slot width of 1 mm. Both the CPW and slotline are designed to possess a characteristic impedance of 100 Ω around the designed center frequency of 2 GHz according to the closed-form formulas in [1]. The four-finger interdigital capacitor in this case has a finger width of 0.5 mm, a finger length of 3.4 mm, and a gapwidth of 0.2 mm. For the shorted slotline section, its length and width are 4.8 and 1 mm, respectively. The total area occupied by this parallel LC circuit is about $(\lambda/28)\cdot(\lambda/12)$, and this transition structure is obviously much smaller than the conventional ones using the $\lambda/4$ transformer structures.

The measurement of transition is done on an HP8510 network analyzer with thru-reflect-line (TRL) calibration to the CPW–slotline junction, and the simulation is based on the equivalent-circuit model [see Fig. 1(b)]. The measured and simulated results are shown in Fig. 2. This transition exhibits a bandpass behavior, as expected, and the 1.5-dB passband is in the 1.96$\sim$3.3-GHz frequency range. Good agreement between the measured and simulated results around the passband is observed. The equivalent capacitance and inductance of this structure are 0.6525 pF and 5.5 nH, respectively. This corresponds to a passband center frequency of $1/(2\pi\sqrt{LC}) \cong 2.66$ GHz, which agrees well with the experimental result. Although there is some discrepancy between measured and simulated results in the higher frequency range, the equivalent-circuit model is still adequate in predicting the transition behavior around the passband. Note that all the components in this model except the shorted slotline end are characterized by closed-form expressions, thus the simulation time may be reduced.

To reduce the size of a lumped-element transition even more, the "ring-type L" CPW-to-slotline transition structure proposed

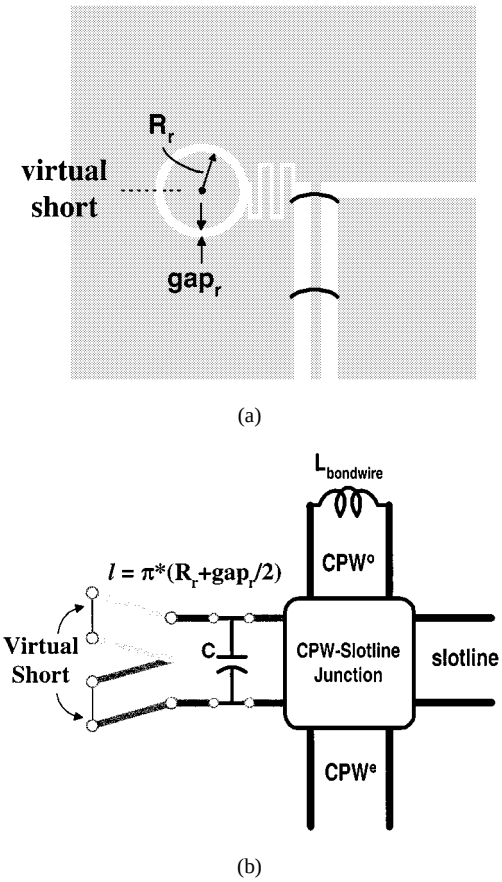

Fig. 3. "Ring-type L" lumped-element CPW-to-slotline transition: (a) layout and (b) equivalent-circuit model.

in [15] and shown in Fig. 3(a) is also examined. Here, two shorted slotline stubs instead of one are connected in series and are arranged to form a slotline ring. Excited with a 180° phase difference, the two slotline stubs are now terminated by ideal short circuits in the equivalent-circuit model [see Fig. 3(b)], and no full-wave simulation is needed. In addition, the size of the transition is further reduced by this realization because the effective inductances of two stubs are added such that each stub can be made shorter, and the slotline stubs are curved such that the horizontal length of the transition is reduced.

Measured and simulated results of this "ring-type L" transition are shown in Fig. 4. This transition is also fabricated on the FR4 substrate, with the same CPW and slotline dimensions as in Fig. 2. The 1.5-dB passband is in the 1.53$\sim$2.76-GHz frequency range, which corresponds to a 1.8 : 1 bandwidth. The equivalent capacitance and inductance values are 0.6525 pF and 5.89 nH, respectively. The corresponding resonance frequency is 2.57 GHz, which again agrees with the measured passband center frequency.

The measured and simulated results for the "ring-type L" transition do not match well. One explanation is that all the discontinuity effects and losses associated with the parallel LC circuit are not taken into consideration. However, this simplified model [see Fig. 3(b)] is still adequate in predicting the frequency range of the transition passband and has the advantage of very short calculation time, a consequence of no full-wave simulation. Thus, it is very suitable for CAD purposes.

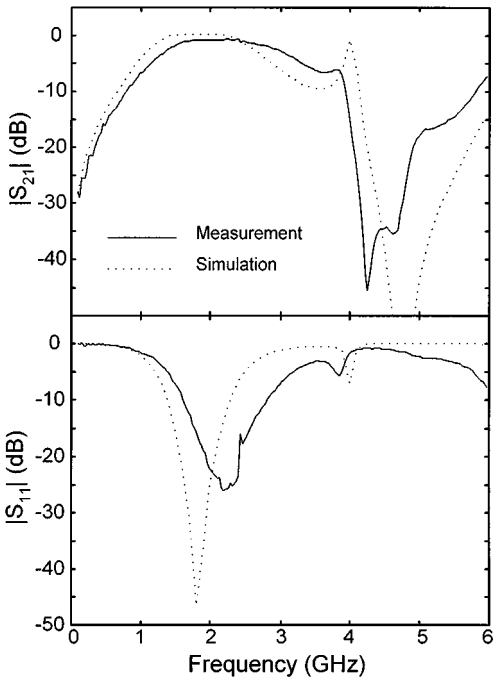

Fig. 4. Measured and simulated results for the back-to-back "ring-type L" lumped-element CPW-to-slotline transition shown in Fig. 3(a). (For L: ring inner radius = 2.5 mm, gapwidth = 0.5 mm; for C: finger length = 3.2 mm, finger width = 0.5 mm, gapwidth = 0.2 mm.)

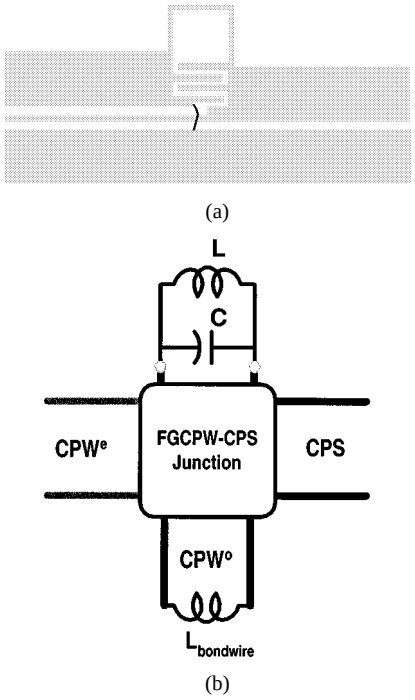

Fig. 5. Basic lumped-element FGCPW-to-CPS transition: (a) layout and (b) equivalent-circuit model.

For the "ring-type L" transition, the size of the interdigital capacitor is about $(\lambda/30)\cdot(\lambda/30)$ and the radius of the slotline ring is $R_r \cong \lambda/36$. The transition size is about 1/12 smaller than the conventional slotline-radial-open transition [8]. This again reveals the effective size reduction capability of lumped-element transition.

III. Basic Lumped-Element FGCPW-to-CPS Transition Structures

By employing the same concept to the FGCPW structure, a lumped-element FGCPW-to-CPS transition [see Fig. 5(a)] can also be implemented. Here the inductor is realized by a section of shorter metal strip whose length is much smaller than the wavelength. The quasi-static closed-form formula associated with the partial-element equivalent-circuit model [18] is adopted for the inductance calculation. The inductance value can be obtained when the strip length, width, thickness, and the conductivity are specified. The equivalent-circuit model of the transition in Fig. 5(a) is shown in Fig. 5(b). Here, the FGCPW–CPS junction model modified from the CPW–slotline one [17] is again included to discuss the mode conversion effect between the even and odd CPW modes.

A back-to-back lumped-element FGCPW-to-CPS transition for Fig. 5(a) is also fabricated on the FR4 substrate. The FGCPW line has a strip width of 0.45 mm, a slot width of 0.6 mm, and a finite ground-plane width of 4 mm. The CPS line has a strip width of 4 mm and a slot width of 0.6 mm. Both FGCPW and CPS lines are designed to possess a characteristic impedance of 100 Ω according to the closed-form formulas in [1]. The four-finger interdigital capacitor in this case has a finger width of 0.5 mm, a finger length of 3.7 mm, and a gapwidth of 0.3 mm. For the shorter metal strip, its length and width are 12.05 and 0.5 mm, respectively. The total area occupied by the parallel LC circuit is about $(\lambda/28)\cdot(\lambda/14)$. The measured and simulated results are shown in Fig. 6, where again a good match between them is observed. The 1.5-dB passband is in the 1.17$\sim$3.41-GHz frequency range. The equivalent capacitance of the interdigital capacitor is 0.597 pF, and the equivalent inductance of the shorter metal strip is 10.35 nH.

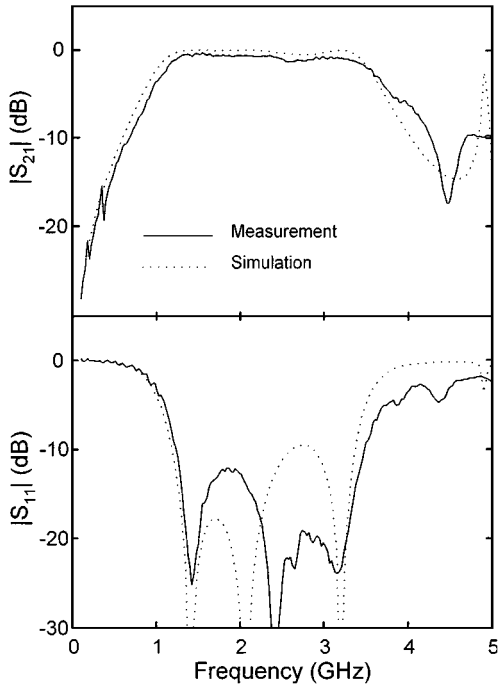

Fig. 6. Measured and simulated results for the back-to-back lumped-element FGCPW-to-CPS transition shown in Fig. 5(a).

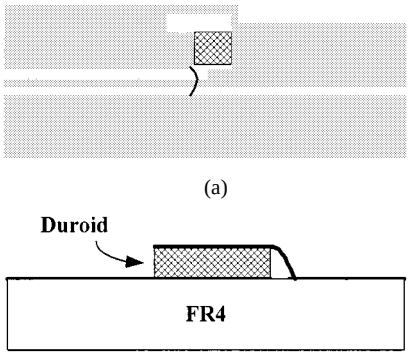

Fig. 7. Lumped-element FGCPW-to-CPS transition designed with MIM capacitor: (a) top view and (b) side view.

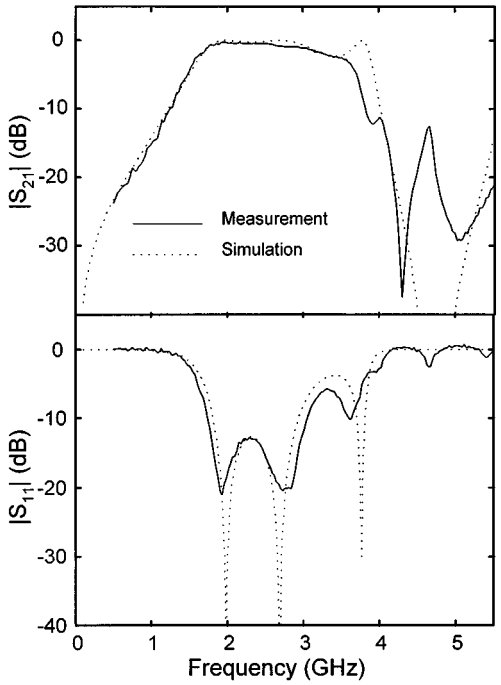

Fig. 8. Measured and simulated results for the back-to-back lumped-element FGCPW-to-CPS transition (Fig. 7) designed with the MIM capacitor.

This corresponds to a center passband frequency of 2.02 GHz, which agrees well with the measured result.

The capacitor in the lumped-element transition may also be realized by a metal–insulator–metal (MIM) configuration. The MIM capacitor structure may achieve a much larger capacitance for a given area compared to its interdigital counterpart. Fig. 7 shows the lumped-element FGCPW-to-CPS transition employing the MIM structure as a capacitor instead of the interdigital capacitor. Characterization of the MIM capacitor may be accomplished by the parallel-plate capacitor formula. A back-to-back lumped-element FGCPW-to-CPS transition based on Fig. 7 is fabricated on the FR4 substrate with the same FGCPW and CPS dimensions as in Fig. 6. Here, the top and bottom metals (2.4 mm $\times$ 3 mm) together with the duroid dielectric ($\varepsilon_r = 10.2$, $\tan\delta = 0.002$, thickness $h = 0.635$ mm) are used to implement the MIM capacitor. This gives a capacitance of 1 pF according to the parallel-plate capacitor formula. The shorter metal strip has a length of 5 mm

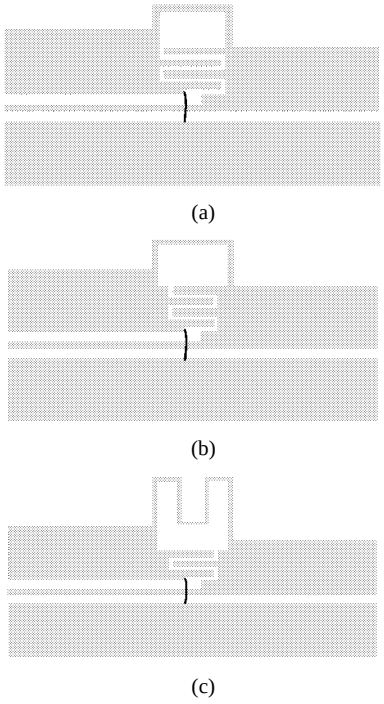

Fig. 9. Layouts of three lumped-element FGCPW-to-CPS transitions designed with same center frequency but with different L and C values. (The relevant geometrical parameters for (a), (b), and (c) are listed in Table I.)

and a width of 0.5 mm, corresponding to an inductance of 3.53 nH. Fig. 8 shows the measured and simulated responses, and a good match between them is observed. The 1.5-dB passband is in the 1.69$\sim$3.1-GHz frequency range. By using the MIM capacitor, an even smaller transition structure can be realized, which is very attractive in implementing the uniplanar MMIC, especially for low-frequency applications.

The bandwidth of the lumped-element transition can be adjusted by suitably choosing the relative values of L and C. Fig. 9 shows the layouts of three FGCPW-to-CPS transitions fabricated on the FR4 substrate with different L and C values. The FGCPW and CPS dimensions are the same as those in Fig. 6. For the metal strips, the width and total length are (a) 0.5 mm, 8.05 mm, (b) 0.3 mm, 9.05 mm, and (c) 0.3 mm, 18.85 mm, respectively. The inductance values for these three cases are 6.27, 8.09, and 14.33 nH, respectively. Note that, for calculating the meander-line inductance in Fig. 9(c), the presence of negative mutual inductances makes the total inductance less than twice that of Fig. 9(b). The interdigital-capacitor structures change accordingly such that the corresponding capacitances are 0.6742, 0.5753, and 0.4374 pF, respectively. This gives the $L \cdot C$ products nearly the same for these three cases, thus the three transitions would be centered at about the same frequency. The relevant geometrical parameters for the three transitions are listed in Table I. Shown in Fig. 10 are the measured results for these three transitions (Fig. 9) in back-to-back configuration. Their passbands are all nearly centered at the same frequency of 2.3 GHz, as expected. However, the 1.5-dB relative bandwidths are 1.8 : 1, 2.25 : 1, and 3 : 1, respectively. As a rule of thumb, the bandwidth of lumped-element transition increases as the inductance value increases. This phenomenon can be predicted from the input impedance characteristics of the parallel

TABLE I
GEOMETRICAL PARAMETERS OF THE FGCPW-TO-CPS TRANSITIONS FOR FIG. 10 (LENGTH UNITS IN MILLIMETERS)

	Interdigital Capacitor				Inductor	
Layout	Finger Number	Finger Length	Finger Width	Gap Width	Strip Length	Strip Width
Fig. 9(a)	4	3.4	0.5	0.3	8.05	0.5
Fig. 9(b)	4	2.6	0.5	0.2	9.05	0.3
Fig. 9(c)	3	2.6	0.5	0.2	18.85	0.3

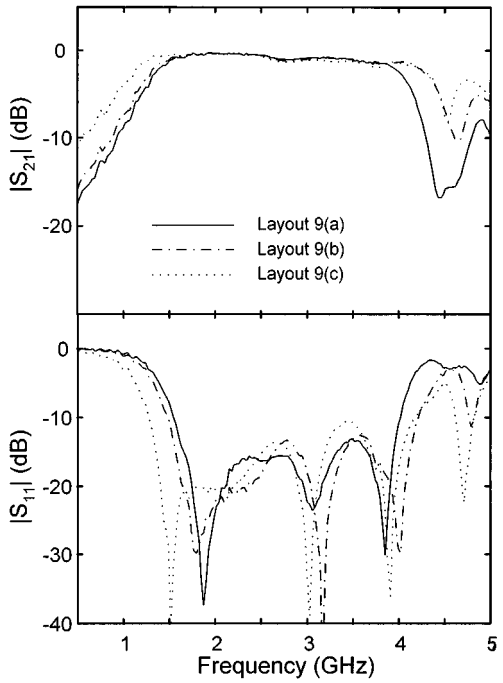

Fig. 10. Measured results for the three back-to-back FGCPW-to-CPS transition structures shown in Fig. 9.

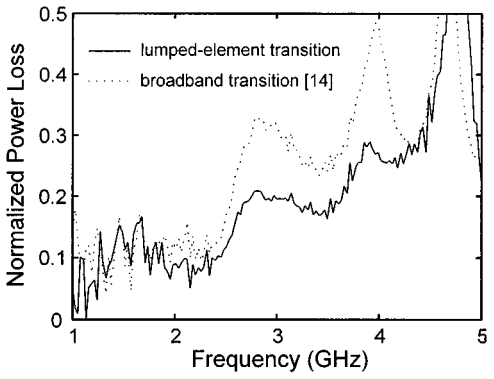

Fig. 11. Measured power losses of the lumped-element transition [see Fig. 9(b)] and broad-band transition in the back-to-back configuration.

LC section, whose magnitude is proportional to L near the resonant frequency.

The measured power loss of the lumped-element FGCPW-to-CPS transition structure in Fig. 9(b) is compared with that of the broad-band CPW-to-CPS transition using a slotline open structure [14] and fabricated on the FR4 substrate. As shown in Fig. 11, the normalized power loss of the lumped-element transition is smaller than that of broad-band one over the passband frequency.

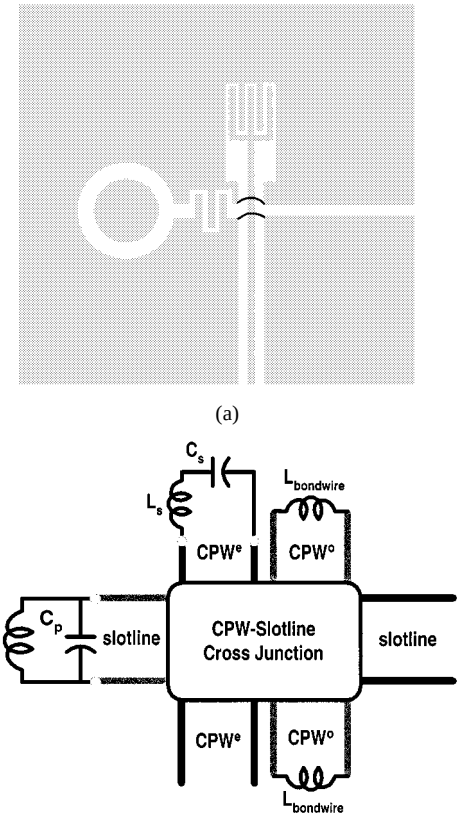

Fig. 12. Lumped-element Marchand-balun-type CPW-to-slotline transition: (a) layout and (b) equivalent-circuit model.

High power loss of a transition might cause unwanted crosstalk to other components in a circuit and degrades the circuit performance. The low-loss characteristic makes the proposed basic lumped-element transitions in Sections II and III feasible for a uniplanar MMIC with high circuit density. These basic lumped-element transitions are also suitable for use as the feeding structure of balanced antennas because of the lower interaction with the antenna, thus a lower level of cross-polarization wave can be expected.

IV. LUMPED-ELEMENT MARCHAND-BALUN TYPE UNIPLANAR TRANSITIONS

Uniplanar transitions can also be implemented using the Marchand-balun structures [8]–[10]. This kind of transition usually has a sharper gain slope, and this characteristic may be used in the design of a filter [8]. However, the conventional Marchand-balun, being composed of $\lambda/4$ open and short stubs, would occupy a large circuit area.

Fig. 12(a) shows the layout of the proposed lumped-element Marchand-balun-type CPW-to-slotline transition. Here, the series and parallel LC circuits, respectively, are used to replace the opened and shorted $\lambda/4$ stubs in the conventional designs [8], [9] so as to minimize the transition size. The parallel LC circuit is composed of an interdigital capacitor (C_p) and a slotline ring structure (L_p) as described in Section II. The series LC circuit is realized by the series connection of a shorter metal

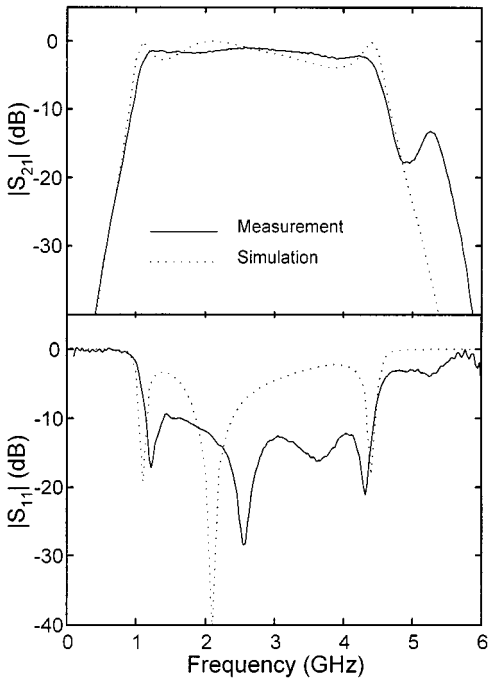

Fig. 13. Measured and simulated results for the back-to-back lumped-element Marchand-balun-type CPW-to-slotline transition shown in Fig. 12(a). (For L_s: strip length $= 5.5$ mm, strip width $= 0.4$ mm; for C_s: finger length $= 2.9$ mm, finger width $= 0.4$ mm, gapwidth $= 0.2$ mm; for L_p: ring inner radius $= 2.1$ mm, gapwidth $= 1$ mm; for C_p: finger length $= 2.2$ mm, finger width $= 0.5$ mm, gapwidth $= 0.3$ mm.)

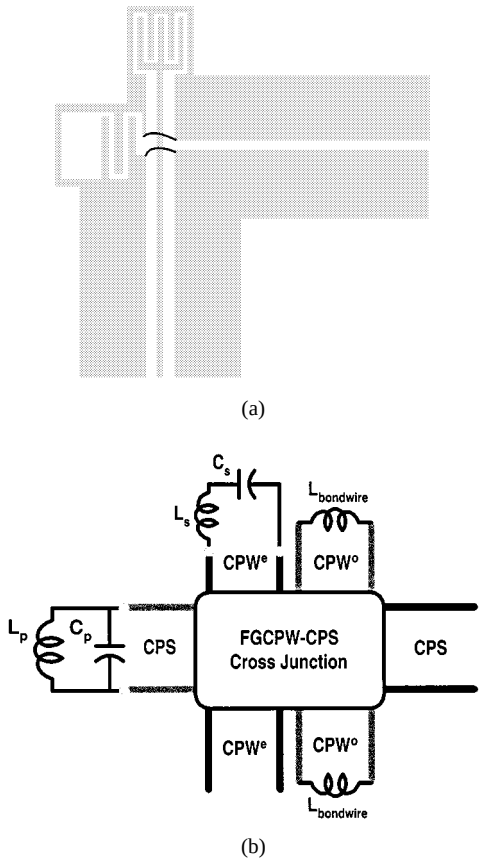

Fig. 14. Lumped-element Marchand-balun-type FGCPW-to-CPS transition: (a) layout and (b) equivalent-circuit model.

strip (L_s) and an interdigital capacitor (C_s). The parallel and series LC circuits are designed such that they are resonant at the same frequency, which is the desired transition center frequency. The equivalent-circuit model shown in Fig. 12(b) is used to discuss the transition characteristics. Here, the CPW-slotline cross-junction model [19] is included to discuss the mode conversion effect at the junction. Again, all the elements in the equivalent circuit can be described by closed-form expressions [16]–[18]; thus, one may save a lot of computation time.

By discarding the cross-junction model, the equivalent-circuit model in Fig. 12(b) may be identified with a second-order bandpass filter. Therefore, the conventional filter synthesis technique can easily be incorporated into the design of a lumped-element Marchand-balun-type transition. Here, the characteristic impedances of the CPW and slotline are equal, thus the second-order maximally flat response is adopted. By giving the desired center frequency f_0, relative 3-dB bandwidth, and transmission-line characteristic impedance, one may obtain the required design values for L_s, C_s, L_p, and C_p by the filter transformation formulas [20]. This may facilitate the design of a lumped-element Marchand-balun-type transition according to a given specification.

A back-to-back lumped-element Marchand-balun-type CPW-to-slotline transition [see Fig. 12(a)] is built on the FR4 substrate, in which the CPW strip width $= 0.45$ mm, the CPW slot width $= 0.6$ mm, and the slotline slot width $= 0.7$ mm. The measured and simulated results are shown in Fig. 13. This transition is designed with a center frequency at 3 GHz, a relative 3-dB bandwidth of 200%, and a transmission-line characteristic impedance of 100 Ω. The required LC structures have the values $L_s = 3.75$ nH, $C_s = 0.75$ pF, $L_p = 7.5$ nH, and $C_p = 0.375$ pF, according to the filter design formulas. The measured transition response (Fig. 13) shows a bandpass behavior, as expected, with a center frequency at 3 GHz. The measured insertion loss is less than 3 dB in the 1.12$\sim$4.38-GHz frequency range. Compared to the transition responses in Figs. 2 and 4, the Marchand-balun-type transition has a sharper gain slope, as expected. Note that the transition response is different from that of the ideal maximum flat response because of its back-to-back configuration and the complex discontinuity effects. The agreement between measured and simulated results is good, and the design of the transition can easily be accomplished by employing the filter synthesis formulas together with the proposed equivalent-circuit model. The sizes of parallel and series LC structures in this case are about $(\lambda/7) * (\lambda/10)$ and $(\lambda/8) * (\lambda/12)$, respectively, making the transition much smaller than the conventional ones.

Based on the filter synthesis formulas, the transitions with different bandwidths can easily be realized. Fig. 14(a) shows the layout of the lumped-element Marchand-balun-type FGCPW-to-CPS transition. Its corresponding equivalent-circuit model is shown in Fig. 14(b). Here, a shorter metal strip is used to realize the inductor L_p in the parallel LC circuit as in Section III. Three transitions based on this layout are fabricated on the FR4 substrate with the same FGCPW and CPS dimensions as in Fig. 6. They are designed with the same center frequency of $f_0 = 3$ GHz and line impedance of 100 Ω, but with different 3-dB bandwidths of 100%, 200%, and 300%. Their corresponding L

TABLE II
GEOMETRICAL PARAMETERS OF THE FGCPW-TO-CPS TRANSITIONS FOR FIG. 15 (LENGTH UNITS IN MILLIMETERS)

	Interdigital Capacitor					Inductor		
BW (%)		Finger Number	Finger Length	Finger Width	Gap Width		Strip Length	Strip Width
100	C_s	5	1.9	0.4	0.4	L_s	8.5	0.3
	C_p	5	3.4	0.5	0.2	L_p	5.3	0.5
200	C_s	5	4.1	0.5	0.3	L_s	5.5	0.45
	C_p	3	3	0.5	0.3	L_p	9.3	0.5
300	C_s	7	3.8	0.5	0.2	L_s	3.9	0.5
	C_p	3	2.2	0.4	0.4	L_p	12.75	0.5

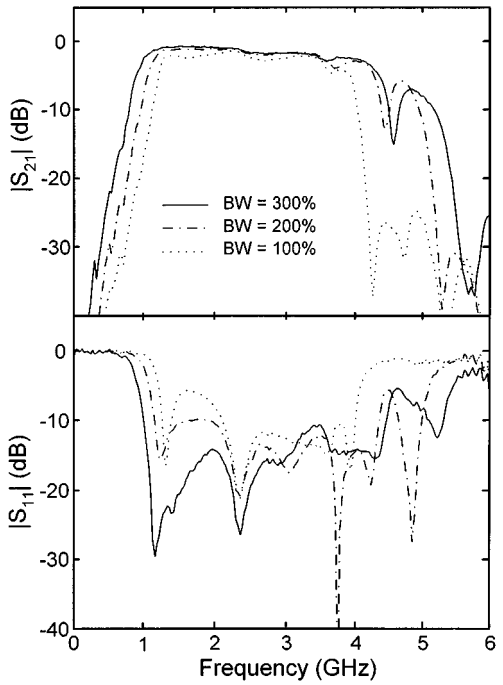

Fig. 15. Measured results for the three back-to-back lumped-element Marchand-balun-type FGCPW-to-CPS transitions shown in Fig. 14(a).

and C values are again calculated by the filter formulas for a second-order maximum flat response, with the relevant geometrical parameters summarized in Table II. Fig. 15 shows the measured results for these three transitions in a back-to-back configuration. Their passbands are all nearly centered at the same frequency of 3 GHz, as expected, and the 3-dB bandwidths are $2.6:1$, $3:1$, and $4:1$, respectively. The measured bandwidths do not match with the designed ones, due to the back-to-back configuration and the complex parasitic effects associated with the discontinuities in the transition structure.

Basically, the proposed lumped-element Marchand-balun-type uniplanar transitions may be regarded as the combination of an unbalanced-to-balanced line transition and a bandpass filter. When this type of transition is used as a balun in a balanced mixer, for example, it has the advantages of small size as well as saving one additional filter. This makes the proposed lumped-element Marchand-balun-type uniplanar transitions particular suitable for use in uniplanar MMICs.

V. CONCLUSION

In this study, novel lumped-element transitions between unbalanced and balanced uniplanar lines have been proposed. Base on this concept, various lumped-element CPW-to-slotline and FGCPW-to-CPS transition structures have been implemented and carefully examined. For the basic lumped-element uniplanar transitions, the center frequency and bandwidth can easily be determined and controlled by an adjustment of L and C values. The lumped-element Marchand-balun-type uniplanar transitions may easily be characterized by adopting the conventional filter synthesis formulas. For design and modeling purpose, effective and simple equivalent-circuit models have also been established. The proposed lumped-element transitions have the merits of very compact size, low power losses, moderate bandwidth, and easy characterization, thus providing simple and effective interconnections between CPW and slotline/CPS. They are attractive in implementing the uniplanar MMIC components.

REFERENCES

[1] K. C. Gupta, R. Garg, I. Bahl, and P. Bhartia, *Microstrip Lines and Slotlines*, 2nd ed. Norwoodl, MA: Artech House, 1996, ch. 5 and 7.
[2] M. Riaziat, R. Majidi-Ahy, and I.-J. Feng, "Propagation modes and dispersion characteristics of coplanar waveguides," *IEEE Trans. Microwave Theory Tech.*, vol. 38, pp. 245–251, Mar. 1990.
[3] L. Fan and K. Chang, "Uniplanar power dividers using coupled CPW and asymmetrical CPS for MIC's and MMIC's," *IEEE Trans. Microwave Theory Tech.*, vol. 44, pp. 2411–2419, Dec. 1996.
[4] F. L. Lin, C. W. Chiu, and R. B. Wu, "Coplanar waveguide bandpass filter—A ribbon of brick wall design," *IEEE Trans. Microwave Theory Tech.*, vol. 43, pp. 1589–1596, July 1995.
[5] L. Fan, B. Heimer, and K. Chang, "Uniplanar hybrid couplers using asymmetrical coplanar strip lines," in *IEEE MTT-S Int. Microwave Symp. Dig.*, 1997, pp. 273–276.
[6] D. Cahana, "A new coplanar waveguide/slotline double-balanced mixer," in *IEEE MTT-S Int. Microwave Symp. Dig.*, 1989, pp. 967–968.
[7] Y.-D. Lin and S.-N. Tsai, "Coplanar waveguide-fed uniplanar bow-tie antenna," *IEEE Trans. Antennas Propagat.*, vol. 45, pp. 305–306, Feb. 1997.
[8] C.-H. Ho, L. Fan, and K. Chang, "Experimental investigations of CPW-slotline transitions for uniplanar microwave integrated circuits," in *IEEE MTT-S Int. Microwave Symp. Dig.*, 1993, pp. 877–880.
[9] K. Hettak, N. Dib, A. Sheta, A. A. Omar, G.-Y. Delisle, M. Stubbs, and S. Toutain, "New miniature broad-band CPW-to-slotline transitions," *IEEE Trans. Microwave Theory Tech.*, vol. 48, pp. 138–146, Jan. 2000.
[10] V. Trifunović and B. Jokanović, "Review of printed Marchand and double Y baluns: Characteristics and application," *IEEE Trans. Microwave Theory Tech.*, vol. 42, pp. 1454–1462, Aug. 1994.
[11] K.-P. Ma and T. Itoh, "A new broadband coplanar waveguide to slotline transition," in *IEEE MTT-S Int. Microwave Symp. Dig.*, 1997, pp. 1627–1630.
[12] Y.-S. Lin and C. H. Chen, "Design and modeling of twin-spiral coplanar waveguide-to-slotline transitions," *IEEE Trans. Microwave Theory Tech.*, vol. 48, pp. 463–466, Mar. 2000.
[13] L. Zhu and K. Wu, "Hybrid FGCPW/CPS scheme in the building block design of low-cost uniplanar and multilayer circuit and antenna," in *IEEE MTT-S Int. Microwave Symp. Dig.*, 1999, pp. 867–870.
[14] S.-G. Mao, C.-T. Hwang, R.-B. Wu, and C. H. Chen, "Analysis of coplanar waveguide-to-coplanar stripline transitions," *IEEE Trans. Microwave Theory Tech.*, vol. 48, pp. 23–29, Jan. 2000.
[15] Y.-S. Lin and C. H. Chen, "Novel lumped-element coplanar waveguide-to-slotline transitions," in *IEEE MTT-S Int. Microwave Symp. Dig.*, 1999, pp. 1427–1430.
[16] S. S. Gevorgian, T. Martinsson, L. J. P. Linner, and E. L. Kollberg, "CAD models for multilayered substrate interdigital capacitors," *IEEE Trans. Microwave Theory Tech.*, vol. 44, pp. 896–904, June 1996.
[17] M. Ribo, J. de la Cruz, and L. Pradell, "Circuit model for slotline-to-coplanar waveguide asymmetrical transitions," *Electron. Lett.*, vol. 35, pp. 1153–1155, July 8, 1999.

[18] A. E. Ruehli, "Inductance calculations in a complex integrated circuit environment," *IBM J. Res. Develop.*, vol. 16, pp. 470–481, Sept. 1972.
[19] M. Ribo and L. Pradell, "Circuit model for a coplanar-slotline cross," *IEEE Microwave Guided Wave Lett.*, vol. 10, pp. 511–513, Dec. 2000.
[20] G. L. Matthaei, L. Young, and E. M. T. Jones, *Microwave Filters, Impedance-Matching Networks, and Coupling Structures*. Norwood, MA: Artech House, 1980.

Yo-Shen Lin was born in Taipei, Taiwan, R.O.C., in 1973. He received the B.S. and M.S.E.E. degrees in electrical engineering from the National Taiwan University, Taipei, Taiwan, R.O.C., in 1996 and 1998, respectively, and is currently working toward the Ph.D. degree in communication engineering at the National Taiwan University.

His research interests include the design and analysis of microwave circuits and systems.

Chun Hsiung Chen (SM'88–F'96) was born in Taipei, Taiwan, R.O.C., on March 7, 1937. He received the B.S.E.E. and Ph.D. degrees in electrical engineering from the National Taiwan University, Taipei, Taiwan, R.O.C., in 1960 and 1972, respectively, and the M.S.E.E. degree from the National Chiao Tung University, Hsinchu, Taiwan, R.O.C., in 1962.

In 1963, he joined the Faculty of the Department of Electrical Engineering, National Taiwan University, where he is currently a Professor. From August 1982 to July 1985, he was Chairman of the Department of Electrical Engineering at the National Taiwan University. From August 1992 to July 1996, he was the Director of the University Computer Center. In 1974, he was a Visiting Scholar in the Department of Electrical Engineering and Computer Sciences, University of California at Berkeley. From August 1986 to July 1987, he was a Visiting Professor in the Department of Electrical Engineering, University of Houston, Houston, TX. In 1989, 1990, and 1994, he visited the Microwave Department, Technical University of Munich, Munich, Germany, the Laboratoire d'Optique Electromagnetique, Faculte des Sciences et Techniques de Saint-Jerome, Universite d'Aix-Marseille III, France, and the Department of Electrical Engineering, Michigan State University, East Lansing, respectively. His areas of interest include microwave circuit analysis and computational electromagnetics.